Thus we have four lines of evidence that sperm initiate the fertilization potential by means of acrosomal protein: (i) acrosomal protein is in intimate contact with the oocyte surface at the time of fertilization (*11*), (ii) the isolated protein causes a fertilization potential–like response, (iii) sperm initiate fertilization potentials in the probable absence of fusion, and (iv) sperm lipids are not required. It will be interesting to determine whether blocking the acrosomal protein on sperm will prevent induction of fertilization potentials.

If sperm-egg fusion does not open the fertilization potential channels, the most likely mechanism is that molecules on the sperm surface (for example, the acrosomal protein in *Urechis*) interact with egg surface components to open the channels. This interaction could be of a specific receptor-ligand nature, although other possibilities can be envisaged. Sperm surface molecules could open egg membrane channels by modifying the egg surface charge or by inserting into the egg bilayer, changing its structure. Both possibilities are reasonable for acrosomal protein which is a polycation and has hydrophobic properties (*11*). In *Urechis* it is also known that the fertilizing sperm opens only a localized patch of Na^+ channels (*18*); thus the acrosomal protein could even be acting directly on the egg membrane without the involvement of a second messenger system.

REFERENCES AND NOTES

1. S. Hagiwara and L. A. Jaffe, *Annu. Rev. Biophys. Bioeng.* **8**, 385 (1979).
2. L. A. Jaffe, *Nature (London)* **261**, 68 (1976).
3. ——— and M. Gould, in *Biology of Fertilization*, C. B. Metz and A. Monroy, Eds. (Academic Press, New York, 1985), vol. 3, pp. 223–250.
4. R. Steinhardt, L. Lundin, D. Mazia, *Proc. Natl. Acad. Sci. U.S.A.* **68**, 2426 (1971).
5. L. A. Jaffe, M. Gould-Somero, L. Z. Holland, *J. Gen. Physiol.* **73**, 469 (1979).
6. N. L. Cross, *Dev. Biol.* **85**, 380 (1981).
7. M. Kozuka and K. Takahashi, *J. Physiol. (London)* **323**, 267 (1982).
8. L. A. Jaffe, M. Gould-Somero, L. Z. Holland, *J. Cell Biol.* **92**, 616 (1982).
9. L. A. Jaffe, N. L. Cross, B. Picheral, *Dev. Biol.* **98**, 319 (1983).
10. L. A. Jaffe and L. C. Schlichter, *J. Physiol. (London)* **358**, 299 (1985).
11. M. Gould, J. L. Stephano, L. Z. Holland, *Dev. Biol.* **117**, 306 (1986). In this work, oocytes activated by protein also developed the slow polyspermy block, but the rapid electrical polyspermy block was not tested for.
12. M. Gould-Somero, L. A. Jaffe, L. Z. Holland, *J. Cell Biol.* **82**, 426 (1979).
13. F. J. Longo, J. W. Lynn, D. H. McCulloh, E. L. Chambers, *Dev. Biol.* **118**, 155 (1986).
14. Chloroform and methanol, 2:1, five washes; chloroform and methanol containing 0.04*N* HCl, seven washes; chloroform and methanol, 1:1, three washes; and methanol, three washes; hydrolysis for 2 hours at 70° to 80°C in methanol containing 2*N* HCl; extraction with hexane; lyophilization of residue (*15–17*).
15. J. Folch-Pi and P. Stoffyn, *Ann. N.Y. Acad. Sci.* **195**, 86 (1972).
16. K. Hantke and V. Braun, *Eur. J. Biochem.* **34**, 284 (1973).
17. G. Marinetti and K. Cattieu, *Biochim. Biophys. Acta* **685**, 109 (1982).
18. M. Gould-Somero, *Nature (London)* **291**, 254 (1981).
19. M. Gould, in *Methods in Developmental Biology*, F. Wilt and N. Wessells, Eds. (Crowell, New York, 1967), pp. 163–171.
20. Artificial seawater (ASW) was 484 m*M* NaCl, 10 m*M* KCl, 27 m*M* $MgCl_2$, 29 m*M* $MgSO_4$, 10 m*M* $CaCl_2$, 2.4 m*M* $NaHCO_3$, *p*H 8. In ASW with 1/10 Ca^{2+}, $CaCl_2$ was 1 m*M*, and in ASW with 1/10 Na^+, NaCl was 49 m*M* with 436 m*M* choline chloride (*5*).
21. Both the hot trichloroacetic acid–extracted acrosomal protein and the major band acrosomal protein extracted from acetic acid–urea polyacrylamide gels (*11*) were used in the experiments; no differences were seen in the oocytes' responses.
22. O. Lowry, N. Rosebrough, A. Farr, R. Randall, *J. Biol. Chem.* **193**, 265 (1951).
23. When oocytes are mixed with a uniform concentration of acrosomal protein, 0.03 mg/ml is sufficient to activate them (*11*).
24. Oscillations in membrane potential during the falling phase of the response are occasionally observed in both fertilization and acrosomal protein potentials.
25. Other criteria for acceptable data were (i) that the Ca^{2+} action potential lasted longer than the stimulus at the beginning of the experiment [when ASW with 1/10 Ca^{2+} was used oocytes were first penetrated with the microelectrode in standard ASW then the Ca^{2+} concentration was changed by perfusion (*5*)] and (ii) that at the termination of the experiment when the electrode was removed from the oocyte into the seawater bath, the zero potential on the chart recorder had not changed by more than ±3 mV from the value before the electrode penetrated the oocyte. These criteria apply to all data in the article.

26. We thank L. Martinez for her help and D. Kline and L. A. Jaffe for comments on the manuscript.

8 September 1986; accepted 27 January 1987

Detection of Rift Valley Fever Viral Activity in Kenya by Satellite Remote Sensing Imagery

KENNETH J. LINTHICUM, CHARLES L. BAILEY, F. GLYN DAVIES, COMPTON J. TUCKER

Data from the advanced very high resolution radiometer on board the National Oceanic and Atmospheric Administration's polar-orbiting meteorological satellites have been used to infer ecological parameters associated with Rift Valley fever (RVF) viral activity in Kenya. An indicator of potential viral activity was produced from satellite data for two different ecological regions in Kenya, where RVF is enzootic. The correlation between the satellite-derived green vegetation index and the ecological parameters associated with RVF virus suggested that satellite data may become a forecasting tool for RVF in Kenya and, perhaps, in other areas of sub-Saharan Africa.

OUTBREAKS OF RIFT VALLEY FEVER (RVF) disease in domestic animals (epizootics) in sub-Saharan Africa are clearly correlated with widespread and heavy rainfall associated with the intertropical convergence zone (*1–4*). It is thought that such rainfall can flood mosquito breeding habitats, known in Kenya as "dambos" (*5*), which contain transovarially infected *Aedes* mosquito eggs and subsequently serve as an excellent habitat for the development of other mosquito vectors (*4, 6, 7*). The introduction of the virus into susceptible vertebrates by *Aedes* and the tremendous increase in numbers of secondary mosquito vectors can create an epizootic of this disease in sub-Saharan Africa. If the rains that evolve from the intertropical convergence zone are not widespread, heavy local rainfall may flood infected mosquito habitats and introduce the virus into domestic vertebrate populations enough to replenish the dambo habitats with infected eggs, but possibly not enough to sustain an epizootic.

To prevent or lessen the impact of RVF disease in Africa, known parameters of epizootic viral activity are monitored so that control efforts can be implemented. Satellite remote sensing technology is the newest and possibly the only method available to conduct surveillance activities over such a large and diversified area as sub-Saharan Africa. Remote sensing of green vegetation dynamics is a well-developed technique and one for which several satellites collect data world-

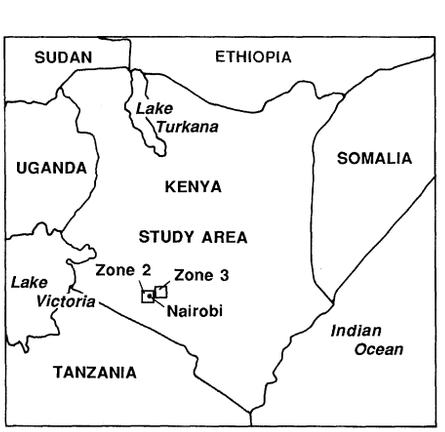

Fig. 1. Location of study areas in Kenya.

K. J. Linthicum and C. L. Bailey, Department of Arboviral Entomology, Disease Assessment Division, U.S. Army Medical Research Institute of Infectious Diseases, Fort Detrick, Frederick, MD 21701–5011.
F. G. Davies, Veterinary Research Laboratory, P.O. Kabete, Kenya.
C. J. Tucker, NASA/Goddard Space Flight Center, Greenbelt, MD 20771.

wide. Such data have been used for surveying ecological conditions predisposed to desert-locust activity (*8, 9*). We analyzed factors related to RVF viral activity and green-leaf vegetation dynamics, with the latter derived from satellite data as they relate directly to rainfall and subsequent vegetation development, during an interepizootic period in a restricted area in Kenya where epizootics occur. We describe a quantifiable detection methodology that could be applied on a continental basis with data from polar-orbiting meteorological satellites.

The two areas in Kenya where RVF virus studies were conducted are described on the basis of the classification of Kenyan ecoclimatic zones one through six (*10*) and are defined in terms of climate and vegetation. The study areas, zones 2 and 3 in Fig. 1, have been described (*7*). Monthly rainfall data were obtained from the Kenya Meteorological Department. Adult mosquito population levels and RVF viral activity were continuously monitored from September 1982 to March 1985 (*7*). Observations of the flooding of potential mosquito vector habitats were made concurrently while monitoring the adult mosquito population.

Digital remote sensing data were produced by the advanced very high resolution radiometer (AVHRR) sensor on polar-orbiting meteorological satellites operated by the National Oceanic and Atmospheric Administration (NOAA). The AVHRR records visible, near-infrared, and thermal channels of the electromagnetic spectrum (*11, 12*). The characteristics of the NOAA AVHRR systems used in this study are listed in Table 1. The normalized difference vegetation index (NDVI) analyzed in this study is a transformation between data from the visible channel (Ch1, 0.58 to 0.68 μm) and near-infrared channel (Ch2, 0.725 to 1.1 μm), and is expressed by

$$\text{NDVI} = (\text{Ch2} - \text{Ch1})/(\text{Ch2} + \text{Ch1}) \quad (1)$$

The NDVI data have been shown to be highly correlated with such vegetation parameters as green-leaf biomass, atmospheric CO_2 draw down, and seasonal rainfall (*8, 12, 13*) and represent the photosynthetic capacity of the area measured (*14*).

Weekly AVHRR data were derived from the global area coverage data that are produced by the on-board processing of large area coverage data (1.1 km by 1.1 km) and subsequently transmitted to receiving stations in Virginia or Alaska (*15*). The satellite data have a grid cell (pixel) size of approximately 15 km by 15 km. Weekly composite data were formed by selecting the highest NDVI for each grid cell location from the daily data for that week. Weekly NDVI data were calculated and mapped to a Mercator projection. The highest value during a 3-week period was selected to represent the 3-week composite for each grid cell location. Data selected in this manner tended to occur near nadir, were largely cloud-free, and were characterized by low-aerosol conditions, which minimize atmospheric scattering (*16*). Compositing was performed on the Hewlett-Packard 1000 and Ramtek image-processing system.

The potential viral activity factor (PVAF) statistic was developed from a methodology

Fig. 2. Plots of AVHRR NDVI and PVAF values, monthly rainfall, and mosquito collections from September 1982 to March 1985 at ecological zone 2. Period of RVF virus activity shown by shaded box.

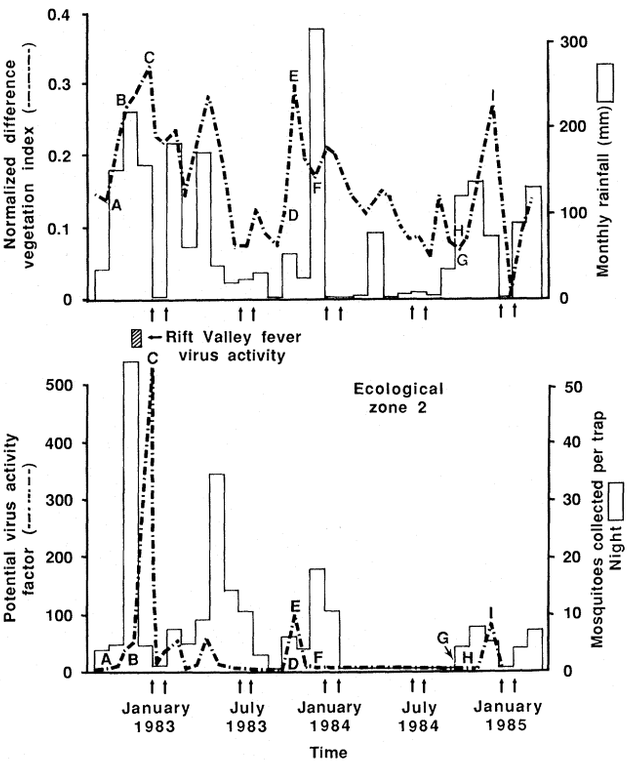

Fig. 3. Plots of AVHRR NDVI and PVAF values, monthly rainfall, and mosquito collections from September 1982 to March 1985 at ecological zone 3. Period of RVF virus activity shown by shaded box.

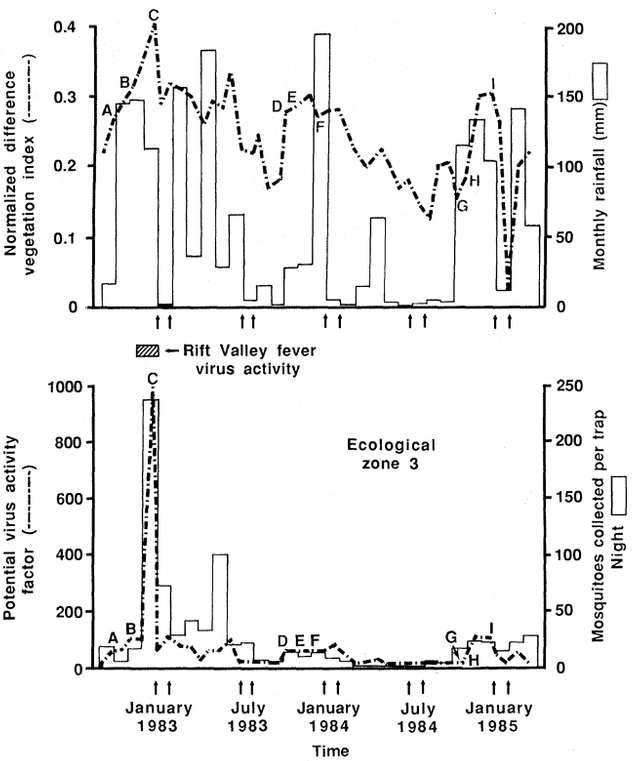

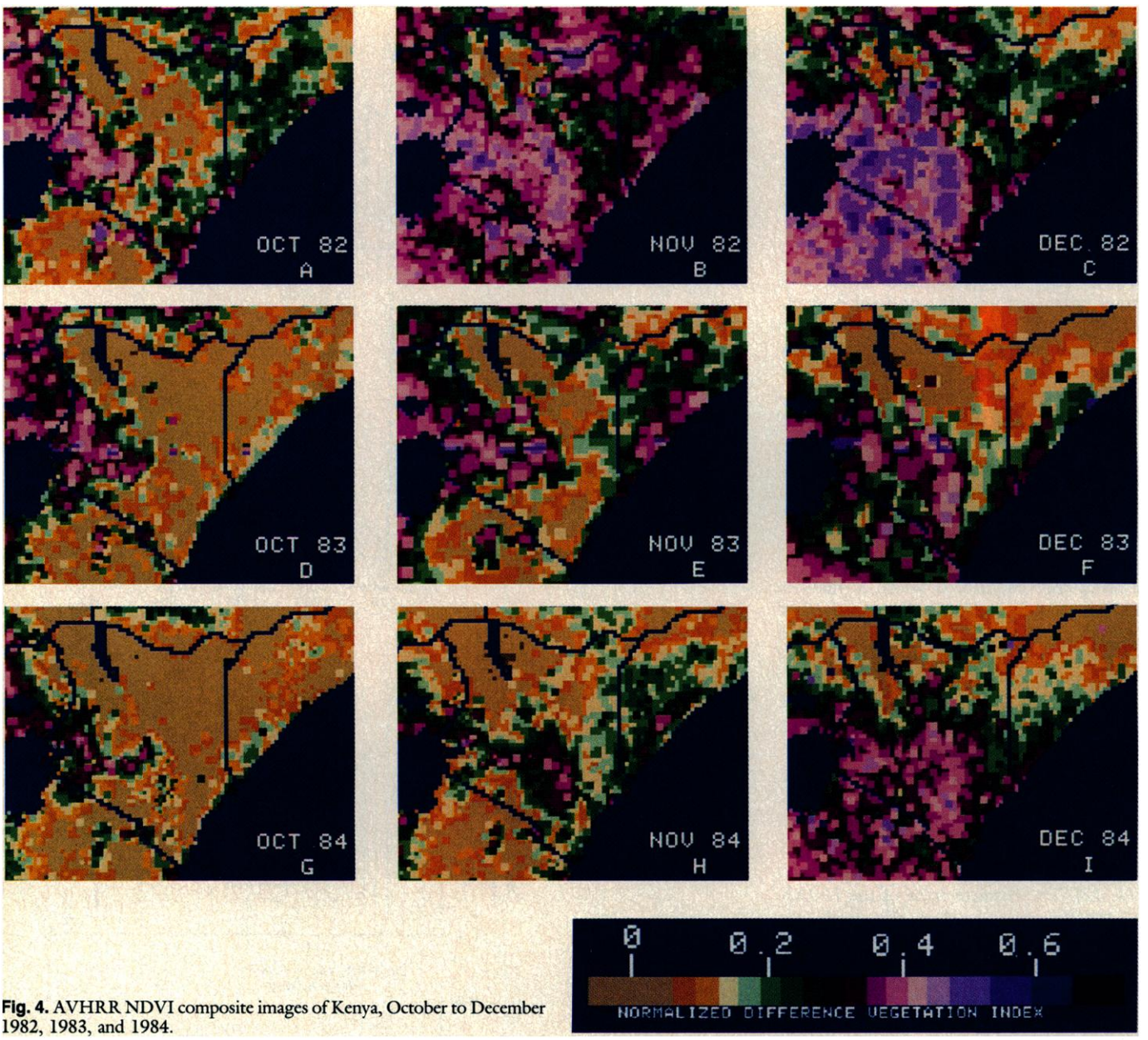

Fig. 4. AVHRR NDVI composite images of Kenya, October to December 1982, 1983, and 1984.

described and tested by Hielkema (*17*) to provide a single indicator of potential desert locust breeding activity. The PVAF progressively weights NDVI classes consistent with field observations that increasing vegetation densities are positively correlated with rainfall, a critical condition to RVF epizootics. The PVAF is calculated from NDVI data by

$$\text{PVAF} = \frac{A\times 10^0 + B\times 10^1 + C\times 10^2 + D\times 10^3}{T} \quad (2)$$

where A is the number of grid cells with $0.05 < \text{NDVI} < 0.20$, B is the number of grid cells with $0.20 < \text{NDVI} < 0.29$, C is the number of grid cells with $0.29 < \text{NDVI} < 0.37$, D is the number of grid cells with $0.37 < \text{NDVI} < 0.65$ [0.65 is the maximum NDVI (*13*)], and $T=4$.

The relation between the NDVI data and the PVAF values and RVF ecological parameters are illustrated in Figs. 2 and 3. During the 31-month study period, rainfall induced the flooding of dambo mosquito breeding habitats once in November and December 1982. This flooding corresponded to the isolation of RVF virus from mosquitoes on 11 occasions (six in zone 2, and five in zone 3).

In both areas, the maximum NDVI and PVAF values were recorded at the period starting 27 December 1982 (point C, Figs. 2 and 3), just following the most consistently rainy 3-month period (October, November, and December 1982) of the 31-month study period. These high values either coincided with (zone 3, Fig. 3) or just followed (zone 2, Fig. 2) the period of maximum mosquito vector populations and RVF viral activity.

Figure 4 presents NDVI images of Kenya for October, November, and December 1982 through 1984. Since NDVI represents a bounded ratio, values can range from −1 to 1. We have assigned brown, gold, green, red, pink, blue, and purple colors to increasing NDVI values from 0.0 to 0.6 as indicated by the color coding bar on Fig. 4. The letters on each of the images correspond to letters indicated on Figs. 2 and 3. The intense pink and blue colors in the December 1982 (C, Fig. 4) image in the central portion of Kenya clearly stand out as the time of most intense green vegetation development, substantially higher than the corre-

Table 1. Characteristics of the NOAA/AVHRR systems. The NOAA-7 satellite was launched in June 1981 and taken out of operation 28 January 1985. NOAA-9 was launched in December 1984 and is still operational.

Characteristic	Measure
Coverage cycle	9 days
Scan angle range	±56°
Ground coverage	2700 km
Orbit inclination	98.9°
Orbital height	833 km
Orbital period	102 min
Ground resolution	1.1 km (nadir); 2.4 km (maximum off-angle along track) 6.9 km (maximum off-angle across track)
Equatorial crossing	Descending mode, 1430 hours Ascending mode, 0230 hours

sponding period in the two subsequent years (F and I, Fig. 4). The December 1982 visual image correlates with the highest NDVI and PVAF values seen at point C (Figs. 2 and 3) and coincides with the only RVF viral activity detected.

The positive correlation between NDVI and rainfall is evident in both ecological zones examined, even though other parameters controlling vegetation production, such as temperature and evapotranspiration, were not considered. In addition, the correlation between NDVI and mosquito populations, as reflected by our collection data, further corroborates the relation between NDVI and rainfall, as mosquito population levels are known to be highly related to rainfall patterns.

The ability of the PVAF to detect, with precision, RVF viral activity in ecological zones 2 and 3 in our study areas during an interepizootic period suggests that RVF epizootics could be detected reliably from this statistic. The isolation of virus in mosquitoes represents the earliest stages in a RVF epizootic. Detection of viral activity at this point in the RVF viral life cycle could allow time for specific control operations before an epizootic occurs. The PVAF generates rapid knowledge about potential viral activity conditions in ecologically equivalent areas and consolidates NDVI data, effectively reducing the operational decision-making process as it relates to control strategies. The ground studies and remote sensing technology discussed here for RVF virus will certainly have an application to other diseases that decimate the continent and are ecologically linked, either directly or through transmission vectors.

REFERENCES AND NOTES

1. R. Swanepoel, in *Contributions to Epidemiology and Biostatistics: Rift Valley Fever*, M. A. Klingberg, Ed. (Karger, Basel, 1981), vol. 3, pp. 83–91.
2. B. M. McIntosh and P. G. Jupp, in *ibid.*, pp. 92–99.
3. F. G. Davies and R. B. Highton, *Trans. R. Soc. Trop. Med. Hyg.* **74**, 815 (1980).
4. F. G. Davies, K. J. Linthicum, A. D. James, *Bull. WHO* **63**, 941 (1985).
5. E. Ackermann, *Wiss. Veroff. Mus. Landerk. Leipzig* **4**, 147 (1936).
6. K. J. Linthicum, C. L. Bailey, F. G. Davies, A. Kairo, *Bull. Entomol. Res.* **75**, 661 (1985).
7. K. J. Linthicum, F. G. Davies, A. Kairo, C. L. Bailey, *J. Hyg.* **95**, 197 (1985).
8. C. J. Tucker, J. U. Hielkema, J. Roffey, *Int. J. Remote Sens.* **6**, 127 (1985).
9. J. U. Hielkema, J. Roffey, C. J. Tucker, *ibid.* **7**, 1609 (1986).
10. D. J. Pratt, P. J. Greenway, M. D. Gwynne, *J. Appl. Ecol.* **3**, 369 (1966).
11. H. Schwalb, *NOAA (Nat. Oceanic Atmos. Adm.) Tech. Memo NESS 95*, (1982).
12. C. O. Justice, J. R. G. Townshend, B. N. Holben, C. J. Tucker, *Int. J. Remote Sens.* **6**, 1271 (1985).
13. C. J. Tucker, J. R. G. Townshend, T. E. Goff, *Science* **227**, 369 (1985).
14. P. J. Sellers, *Int. J. Remote Sens.* **6**, 1335 (1985).
15. J. D. Tarpley, S. R. Schneider, R. L. Money, *J. Climate Appl. Meteorol.* **23**, 491 (1984).
16. B. N. Holben and R. S. Fraser, *Int. J. Remote Sens.* **5**, 145 (1984).
17. J. U. Hielkema, *FAO Tech. Rep. CGP/INT/349/USA* (1980).

18. We thank the staff of the Veterinary Research Laboratory Kabete for technical assistance. The satellite portion of this research was funded by NASA's Life Sciences.

5 September 1986; accepted 13 January 1987

Signaling for Growth Orientation and Cell Differentiation by Surface Topography in *Uromyces*

HARVEY C. HOCH, RICHARD C. STAPLES, BRIAN WHITEHEAD, JERRY COMEAU, EDWARD D. WOLF

The dimensions of the topographical signals for growth orientation and infection structure formation, a cell differentiation event that includes nuclear division, were determined for the stomatal penetrating rust fungus *Uromyces appendiculatus*. The differentiation signal was found to be a simple ridge on the substrate surface that had a markedly optimum height of 0.5 micrometer. Such ridges were microfabricated on silicon wafers by using electron-beam lithography. A similar ridge, in the form of a stomatal lip, was found associated with the stomatal guard cells of the bean (*Phaseolus vulgaris*) leaf. Ridge elevations greater than 1.0 micrometer or less than 0.25 micrometer did not serve as effective signals. Germ tubes of the fungus were highly oriented by ridge spacings of 0.5 to 6.7 micrometers. The data indicate that the fungus is able to distinguish uniquely minute differences in leaf surface topography in order to infect the host plant.

A BROAD RANGE OF EUKARYOTIC cells sense surface signals (*1, 2*), but none display a more precise and unique recognition phenomenon than that exhibited for topographical perception by many of the obligate fungal plant pathogens (*3–5*). For example, the bean rust fungus, *Uromyces appendiculatus* (Pers.) Unger, germinates from a spore and grows on the leaf surface as a hypha in a precisely oriented direction toward a stomate where it ceases growth and develops a series of specialized infection structures necessary for leaf colonization (*5, 6*). The developmental sequence involves gene expression (*7*), mitosis, and distinct morphological changes (*8*). The first of these infection structures, termed an appressorium, forms directly over the stomate (Fig. 1) through which it must eventually enter the leaf to develop other infection structures, for example, vesicles, haustorial mother cells, and haustoria. Using chemically inert plastic replicas of the leaf surface, Wynn (*9*) showed that the precise positioning of the appressorium over the stomate was solely in response to topographical features inherent on the stomatal guard cells. It was thought that a sequence of topographical signals was required to trigger this event (*4*); however, Staples *et al.* recently demonstrated that only a single scratch in the substrate was necessary (*5*). The nature, size, and location of these topographical signals have until now only been surmised.

During investigations to create artificial substrates that are reproducibly inductive for appressorium formation, we discovered that *U. appendiculatus* recognizes, to a very high degree, a topography formed by the leading edge of a sharply inclined raised surface. The inductiveness of the elevated surface edge was directly related to its height. We further determined that a similar topography is present on the stomatal guard cell, and undoubtedly is the signal that the fungal cell perceives to undergo cell differentiation before invasion of the host.

H. C. Hoch, Department of Plant Pathology, New York State Agricultural Experiment Station, Cornell University, Geneva, NY 14456.
R. C. Staples, Boyce Thompson Institute for Plant Research, Cornell University, Ithaca, NY 14853.
B. Whitehead, J. Comeau, E. D. Wolf, National Research and Resource Facility for Submicron Structures, Cornell University, Ithaca, NY 14853.